RSC Advances

ROYAL SOCIETY OF CHEMISTRY

www.rsc.org/advances

Fabrication and evaluation of nanofibrous membranes with photo-induced chemical and biological decontamination functions

Jing Zhu and Gang Sun*

Fiber and Polymer Science, University of California, Davis, CA 95616, United States

Abstract

Hydrophilic nanofibrous membranes with photo-induced self-cleaning functionals were successfully prepared by covalently incorporating a photo-active anthraquinone derivative onto the surfaces of poly(vinyl alcohol-*co*-ethylene) (PVA-*co*-PE) nanofibrous membranes. The presence of the formation of ester bonds between anthraquinone structures and nanofiber surfaces from ATR-FTIR results confirmed the desired surface functionalization. SEM images revealed that prepared membranes possessed uniform nanofibers and ultrafine porous structures and it remained intact after surface functionalization. Under UVA irradiation, these photo-active compound modified nanofibrous membranes are capable to generate reactive oxygen species (ROS), which attributes to the observed self-decontamination functions. The generation of ROS was evaluated via quantitative determination of hydrogen peroxide on the membrane surfaces by using an iodometric titration method. The prepared hydrophilic nanofibrous membranes exhibited powerful photo-induced chemical and biological decontamination functions, including over 99.999% of reduction against both *E. coli* and *S. aureus*, and a total decontamination of aldicarb, a carbamate pesticide, under light irradiation within a short contact time.

Keywords: nanofibrous membranes, anthraquinone-2-carboxylic acid, photo-induced activity, chemical and biological decontamination

Corresponding author: Gang Sun, Tel.: (530)752-0840; Fax: (530)752-7584;

Email: gysun@ucdavis.edu

Introduction

The protection of professionals of health care, chemical and agriculture productions and military personnel from pathogenic microorganisms and toxic chemicals has inspired research activities on advancements of protective functional materials.[1-7] As an effort of producing light weight, breathable and comfortable protective clothing materials, there is a growing interest in exploring nanofibrous membranes as physical barriers to both biological hazards and chemical toxins owing to their intrinsic properties in terms of ultrafine pore size, highly open porous structure and extraordinary high surface area. Such structural features also exhibit excellent resistance to convective gas flow as well as high vapor transmission rate, making nanofibrous membranes ideal materials for protective application.[8-13] However, as a result of the absence of active functional groups, conventional nanofibrous membranes usually only can serve as barriers against large size microorganisms and particles, but still could carry them on the outside surfaces, which may further contribute to secondary contaminations.[14, 15] Therefore, it is highly desirable to introduce chemical and biological decontaminating functions into nanofibrous membranes to offer improved personal protections.

Considerable efforts have been devoted to achieve chemical and biological decontamination functions of nanofibrous membranes.[14] Among these technologies, photo-active agents have attracted great attention in recent years, since they are capable of generating reactive oxygen species (ROS), such as hydroxyl radicals, singlet oxygen and superoxide. These on-site produced ROS are oxidative agents that could kill microorganisms and oxidatively decompose certain toxic chemicals.[16-22] Such properties make photo-active agents applicable in water and air purification, chemical and biological protective clothing materials.[23] Specifically, inorganic photo-sensitizers, such as titanium oxide, zinc oxide and magnesium oxide, were incorporated onto different textiles and nanofibrous membranes via

both chemical and physical processes to offer desired photoactive properties.[24-28] Unfortunately, physically embedded photo-active substances could be substantially released from material matrixes during certain usage periods, which may shorten their life time as functional materials. In addition, since only the functional groups on material surfaces could effectively produce ROS, incorporation of these functional agents underneath matrixes may also weaken their photo-induced functions.[29] Therefore, covalent immobilization of these functional agents onto material surfaces, particularly these with ultrahigh surface area, such as nanofibrous materials, offers a potential pathway to achieve effective and durable photo-active functions. Recently, anthraquinone derivatives were found capable to generate reactive oxygen under UVA or visible light irradiation.[30, 31] Conventional textile materials modified with these photo-active compounds exhibited photo-induced antibacterial and decoloration properties.[32, 33] It can be envisioned that through covalent attachment of anthraquinone moieties onto the surfaces of nanofibrous membranes, a novel self-decontaminating material can be achieved.

To fulfill this goal, three hydrophilic nanofibrous membranes from PVA-*co*-PE polymers with ethylene content at 27, 32, and 44 mol%, individually, were fabricated, whose surfaces were subsequently functionalized with activated anthraquinone-2-carboxylic acid via a facile esterification reaction. The photo-induced antibacterial activities of these prepared membranes were evaluated via challenging these membranes against both *Escherichia coli* (*E. coli*, gram-negative bacterium) and *Staphylococcus aureus* (*S. aureus*, gram-positive bacterium). Moreover, their chemical detoxification properties under UVA irradiation were investigated by decomposing a carbamate pesticide, aldicarb, under various aldicarb concentrations and contact times.

Experiment

1. Materials

Poly(vinyl alcohol-*co*-ethylene) (PVA-*co*-PE, ethylene content 27, 32 and 44 mol %, respectively) and anthraquinone-2-carboxylic acid (AQC) were purchased from Sigma-Aldrich (Milwaukee, WI, USA). Cellulose acetate butyrate (CAB, butyryl content 35-39%), pyridine, acetic anhydride, N,N-carbonyldiimidazole (CDI), acetone and N,N-dimethylformamide (DMF) were supplied by Acros Chemical (Pittsburg, PA, USA). All chemicals were used as received.

2. Preparation of PVA-*co*-PE nanofibrous membranes

PVA-*co*-PE nanofibers were prepared according to a previously published procedure.[34] Briefly, cellulose acetate butyrate (CAB) as a sacrificial matrix was mixed with PVA-*co*-PE in a blend ratio of CAB/PVA-*co*-PE = 80/20, which was gravimetrically fed into a Leistritz co-rotating twin-screw (18 mm) extruder (Model MIC 18/GL 30D, Nurnberg, Germany) at a feed rate of 12 g/min. The blends were extruded into composite fibers through a two strand (2 mm in diameter) rod die, hot-drawn by a take-up device with a drawing ratio of 25 (the area of cross section of the die to that of the extrudates) and air cooled to room temperature. And then, PVA-*co*-PE nanofibers were obtained via soxhlet extraction of acetone to remove CAB from the CAB/ PVA-*co*-PE composite fiber. The prepared PVA-*co*-PE nanofibers were subsequently made into suspensions and deposited onto a polyester monofilament fabric as a releasing surface. After evaporation of solvents, PVA-*co*-PE nanofibrous membranes was formed.

3. Determination of hydroxyl groups

Theoretic hydroxyl group content of PVA-*co*-PE polymer was calculated based on individual molar ratio of ethylene content, and practical hydroxyl group content of PVA-*co*-PE nanofiber surfaces was evaluated via an acetic anhydride/pyridine titration method[35]. Typically, 60 mg PVA-*co*-PE nanofibrous membranes was immersed into 10 mL of dry pyridine which is previously mixed with 0.2 mL acetic anhydride. After shaking for 12 hours at 50 °C, 2 mL distilled water was added to convert the excessive acetic anhydride into acetic acid, which was titrated by 0.1 M NaOH. And the titration curves were recorded via a pH meter (848 Titration Plus, Metrohm Swiss). Blank solutions without PVA-*co*-PE nanofibrous membranes were also tested as controls.

4. Surface functionalization of PVA-*co*-PE nanofibrous membranes

AQC compound was covalently attached onto PVA-*co*-PE nanofibrous membranes according to Scheme 1. Concretely, 0.5 mmol of AQC compound was firstly activated with equal amount of N,N-carbonyldiimidazole (CDI) in 20 mL DMF. The mixture was heated to 60 °C for 4 hours, followed by mixing with 30mg of PVA-*co*-PE nanofibrous membranes. After gently shaking overnight, the functionalized membranes were thoroughly washed with DMF (20 mL×2), acetone (20 mL×2), and distilled water (20 mL×2), respectively. The reaction residual and washing solutions were carefully collected together, diluted to 1L and measured by a UV-vis spectrophotometer (Evolution 600, Thermo, USA) at 319 nm. The AQC concentrations of the final solutions were calculated based on a previously established standard calibration curve. The density of immobilized AQC on membrane surfaces was determined by the difference of AQC amounts before and after esterification reactions.

5. Characterizations

Surface morphologies of pristine and surface functionalized PVA-*co*-PE nanofibrous membranes were observed by using a scanning electron microscopy (SEM) (XL 30-SFEG, FEI/Philips, USA) at 5 kV accelerating voltage on gold sputter coated samples. Attenuated total reflectance-Fourier transform infrared spectroscopy (ATR-FTIR) was measured from 1900 to 500 cm^{-1} at a resolution of 4 cm^{-1} by a Nicolet 6700 spectrometer (Thermo Fisher Scientific, USA).

6. Determination of formed hydrogen peroxide on membrane surfaces

An iodometric titration method was applied to determine the amount of generated hydrogen peroxide (H_2O_2) on membrane surfaces.[36] Briefly, 100 mg of membranes were immersed into 20 mL of deionized water, and then 10 mL of 0.2M sulfuric acid and 10 mL of 5% potassium iodide were added to the mixture. After exposed under UVA irradiation for 1 hr, the mixture was titrated by a 0.001 N sodium thiosulfate solution. The end point of titration was determined by monitoring the changes occurring at a redox electrode. Pristine membrane was evaluated as a control. The amount of produced H_2O_2 can be calculated based on the following equation:

$$\mathrm{H_2O_2\ (ppm)} = \frac{1000 \times 17 \times (V_2 - V_1) \times N}{W}$$

where V_2 and V1 are the titration volumes (mL) for the sample and control, respectively. N is the normality of $Na_2S_2O_3$. And W is the weight of membrane samples (g).

7. Antibacterial assessment

Antibacterial properties of surface functionalized PVA-*co*-PE nanofibrous membranes were evaluated by using a modified American Association of Textile Chemist and Colorists (AATCC) Test

Method 100 against both *Escherichia coli* (K-12, *E. coli*, gram-negative bacterium) and *Staphylococcus aureus* (ATCC#12600, *S. aureus*, gram-positive bacterium). Typically, 0.5 mL bacterial suspension with bacterial concentration at 10^5 colony forming units per milliliter (CFU/mL) was applied onto the surface of the AQC functionalized PVA-*co*-PE nanofibrous membranes (50mg) which were placed in a sterilized glass container. The container was irradiated under UVA light (wavelength: 365 nm, light intensity: 1.3~2.0 mW/cm^2) for 30 min and 60 min, respectively, followed by adding 50 mL sterilized distilled water and vigorously shaking for 2 minutes. 0.1 mL of the solution was extracted from the container and exponentially diluted to 10^5 times serially. Subsequently, 0.1 mL of each diluted bacterial suspension was evenly loaded onto a nutrient agar plate and incubated at 37°C for 18 h. The same method was also applied to the pristine PVA-*co*-PE nanofibrous membranes as controls. The percentage reduction of bacteria was calculated according to the following equation:

$$\text{Reduction of Bacteria (\%)} = \frac{A - B}{A} \times 100$$

Where A and B are the number of viable bacteria colonies on the agar plates from the pristine and modified membranes, respectively.

8. Detoxification test

Aldicarb aqueous solution was prepared in concentrations of 0.2 and 0.02 mM. 60 mg of pristine or AQC functionalized PVA-*co*-PE nanofibrous membranes were immersed into each aldicarb solutions, respectively. After irradiation under UVA light (wavelength: 365 nm, light intensity: 1.3~2.0 mW/cm^2) for 3 hours, a volume of 10 uL of each sample was injected into a Waters e2695 HPLC system, equipped with a Waters 2998 photodiode array (PDA) detector (Waters Co., Milford, MA,

USA) for chromatographic studies. Chromatographic separation of aldicarb and degraded products was achieved on a reverse phase C18 column (5 μm particle size, 4.6 by 250mm). HPLC mobile phase was prepared by 60% Milli-Q water and 40% acetonitrile which both contain formic acid (0.1%, v/v) and the flow rate of the mobile phase was set at 0.33 mL/min. The absorbance wavelength was measured ranging from 190 to 800nm. The HPLC system was coupled to Waters Micromass ZQ 2000 (ESI-MS) Mass Spectrometer (MS). The MS was performed under capillary voltage 3000 V, sample cone voltage 60 eV, source temperature 125°C, desolvation temperature 350°C and desolvation gas flow 250 L/h. Micromass MassLynx software (version 4.1) was used for instrument operation and result analysis.

Results and discussion

1. Fabrication of nanofibrous membranes

Poly(vinyl alcohol-*co*-ethylene) (PVA-*co*-PE), a random copolymer of vinyl alcohol and ethylene segments readily available in different blending ratios, possesses good mechanical property, high thermal stability, hydrophilicity and water insolubility.22 Most importantly, the tertiary C-H bonds on secondary alcohol units of PVA-*co*-PE polymer could serve as good hydrogen donors that are required in generation of ROS according to the photo-chemistry of anthraquinone derivatives[30]. In this study, PVA-*co*-PE polymers with ethylene molar ratio at 27, 32 and 44%, respectively, were fabricated into nanofibrous membranes, and their surface morphologies were observed via SEM. As shown in Figure 1 (a, b and c), all three types of membranes are non-woven structure with a large amount of open pores and the nanofiber sizes are ranging from 50 to 350 nm. It is noticeable that the membranes made of PVA-*co*-PE with 44 mol% ethylene content shows a more rough fiber surface, which can be explained

by imperfect coalescence of dispersed PVA-*co*-PE spheres in CAB matrix during the fabrication process.[37]

The feasibility of surface functionalization on nanofibrous membranes is mainly determined by the accessibility and the amount of surface reactive sites. It has been reported that several functional agents have been covalently incorporated to PVA-*co*-PE based materials via chemical modifications of their secondary hydroxyl groups.[38-41] In theory, PVA-*co*-PE polymer containing 27, 32 and 44 mol% ethylene contents have the amounts of hydroxyl groups at 18.4, 17.5 and 15.2 mmol/g, respectively. However, the actual values of PVA-*co*-PE nanofibrous membranes will be much lower since only the surface hydroxyl groups can be accessible. The actual hydroxyl groups are determined as 8.9 and 7.7 mmol/g membrane for PVA-*co*-PE membranes with 27 and 32 mol% ethylene contents, indicating this value decreases as the ethylene contents increase and the vinyl alcohol contents decrease. On the contrary, PVA-*co*-PE membrane with 44 mol% ethylene content shows a higher actual hydroxyl group (9.0 mmol/g membrane) then the other two, which may be a result of its high roughness of nanofiber surfaces (Figure 1c).

2. Surface Functionalization of nanofibrous membranes

In order to incorporate self-cleaning property into PVA-*co*-PE nanofibrous membranes, a organic photo-active compound, anthraquinone-2-carboxylic acid (AQC), was covalently attached onto membrane surfaces. To facilitate this functionalization, a coupling agent, N,N'-carbonyldiimidazole (CDI), was first used to activate AQC compounds via converting their carboxylic acid groups into imidazole carboxylic ester, which then enables their subsequent esterification reactions with hydroxyl groups on membrane surfaces. The AQC functionalized membranes with 27, 32 and 44 mol %

ethylene contents were referred as PVA-*co*-PE27-AQC, PVA-*co*-PE32-AQC and PVA-*co*-PE44-AQC, respectively. The successful immobilization of AQC compounds was confirmed via ATR-FTIR analysis, and the results of AQC compound, pristine PVA-*co*-PE (27 mol% ethylene content) membranes and PVA-*co*-PE27-AQC membranes are presented in Figure 2. The spectrum of functionalized membrane shows two new peaks around 1654 and 1592 cm^{-1}, which are attributed to carbonyl stretching and aromatic C=C stretching from anthraquinone structures. And the results are consistent to the spectrum of AQC compound. In addition, the new peak around 1761 cm^{-1} is associated to carbonyl stretching from a new ester bond formed between AQC compounds and membrane surfaces.[42, 43] The identical ATR-FTIR results were observed for all three types of membrane samples owing to their same polymer structure and subsequent surface functionalizations. The amount of immobilized AQC on membrane surfaces was further evaluated by a UV/Vis method. As shown in Figure 4, PVA-*co*-PE44-AQC membranes possesses the highest AQC loading (0.24 mmol/g membrane), followed by PVA-*co*-PE27-AQC and PVA-*co*-PE32-AQC membranes (0.20 and 0.17 mmol/g nanofiber, respectively). Due to the practicality concern, the stability of these membranes during chemical functionalizations was also evaluated via SEM. No significant difference of their surface morphologies was found (Figure 1 (d, e and f)), suggesting that the introduction of photo-active compounds did not affect the physical morphology of these nanofibrous membranes.

3. Photo-induced activity of AQC immobilized nanofibrous membrane

Previous studies demonstrated that, in the presence of hydrogen donors and oxygen, anthraquinone moieties were capable to generate reactive oxygen species (ROS) under UVA irradiation, which then triggers photo-induced activities of inactivating bacteria, decolorizing textile

colorants and even initiate radical polymerization.[30-33] Herein, we believe that the mechanism of photo-induced reactions of these immobilized AQC structures is the same to the other anthraquinone derivatives reported before due to their structural similarity and the presence of desired hydrogen donor (weak C-H bonds from vinyl alcohol units of PVA-*co*-PE polymer) (Scheme 2). Specifically, the mechanism of this photo-reaction involves three steps, i.e. 1) under UVA irradiation, immobilized AQC structures are excited to their singlet states, which subsequently transfer into triplet states through an intersystem crossing (ISC) process; 2) the triplet excited AQC structures will abstract hydrogen atom from hydrogen donors, the C-H bond of secondary alcohol from PVA-*co*-PE polymer backbone, to produce ketyl radicals; and 3) these radicals will react with oxygen to generate superoxide radical, peroxide radical and hydroxyl radical, which eventually transfer into hydrogen peroxide (H_2O_2).

To quantitatively evaluate the photo activities of AQC immobilized membranes, the amount of formed H_2O_2 was measured by using an iodometric titration method, and the results were presented in Figure 3. As expected, PVA-*co*-PE32-AQC membrane exhibited the lowest amount of H_2O_2 (27 ppm) due to the lowest amount of immobilized AQC. Interestingly, there was no significant difference of H_2O_2 values between PVA-*co*-PE27-AQC (43 ppm) and PVA-*co*-PE44-AQC (42 ppm), even though PVA-*co*-PE44-AQC membrane offers a higher amount of immobilized AQC. As mentioned above, the C-H bonds from secondary alcohol of PVA-*co*-PE polymer act as hydrogen donors to enable the generation of ketyl radicals. Thus, the higher amounts of vinyl alcohol groups in PVA-*co*-PE polymer will facilitate the reaction pathway to produce more ROS. As a result, both two membranes generated a similar level of H_2O_2.

4. Photo-induced antibacterial property

The biocidal activities of three AQC functionalized PVA-*co*-PE nanofibrous membranes were evaluated against both *E. coli* and *S. aureus* according to a modified AATCC 100 method. As shown in Figure 4 and Table 1, all three membranes could kill more than 80% of *E. coli* and 70% of *S. aureus* after exposing to UVA light (365nm) for 30 min. When the irradiation time further increase to 1 hour, no colony of viable bacteria was found on the agar plates for both *E. coli* and *S. aureus* that were exposed onto the AQC functionalized nanofibrous membranes. Meanwhile, proliferated colonies of two bacteria were observed from all pristine membranes under various irradiation durations. Interestingly, the overall reduction rate of *S. aureus* was faster than that of *E. coli* which may be explained by the difference of bacteria structures. It has been reported that longer time is usually required to let biocides to penetrate into the cell wall of *E. coli* than that of *S. aureus* since the cell wall of gram-negative bacteria was overlaid with a supplementary barrier, which does not exist in gram-positive bacteria.[44]

As an effort to study the durability of their photo-induced antibacterial functions, all tested samples were sterilized and thoroughly washed before repeated antimicrobial experiments. Benefiting from the chemical bonding between AQC molecules and membrane surfaces, no noticeable decrease of their antibacterial efficiencies was found after three repeating tests, suggesting that these photo-induced antibacterial properties are durable and reusable.

5. Photo-induced chemical detoxification property

Aldicarb, namely 2-Methyl-2-(methylthio)propanal-*O*-(*N*-methylcarbamoyl)oxime, is a carbamate pesticide and has been widely used as a nematicide in agricultural production.[45] It has been reported

that aldicarb can be oxidized and converted into less toxic compounds in the presence of photosensitizers.[45] In this study, aldicarb was employed as a target toxin to evaluate the photo-induced self-decontamination functions of AQC functionalized PVA-*co*-PE nanofibrous membranes. The pure aldicarb solution, aldicarb solutions immersed with pristine membranes or AQC functionalized membranes were all exposed to UVA irradiation for certain contact time, and then were analyzed via HPLC and mass spectrometer to identify any decomposition or oxidation products.

When the aldicarb concentration was at 0.2 mM (Figure 5(a)), the peak (retention time at 13.14min) was identified as aldicarb due to two natural fragment ions, $[M–OCONHCH3]^+$ at *m/z* 116 and $[M+H_2O]^+$ at *m/z* 208 found from its mass spectrum (Figure 6(a)). For the aldicarb solutions treated with AQC functionalized membranes, the average areas of this peak apparently decreased and the reduction rate followed the order: PVA-*co*-PE32-AQC (20%) < PVA-*co*-PE27-AQC (25%) < PVA-*co*-PE44-AQC (26%). Consistent to the amounts of generated hydrogen peroxide, PVA-*co*-PE32-AQC exhibited the most weak photo-induced oxidative functions. The peak (retention time at 5.41min) is identified as aldicarb sulfoxide, an oxidized product of aldicarb. Though it was overlapped with certain impurity which also existing in the pure aldicarb solution, the average areas of this peak significantly increased from the solutions treated with AQC functionalized membranes. Its mass spectrum is presented in Figure 6(b), with two characteristic peaks, $[M+H]^+$ ion at *m/z* 207 and $[M+H_2O]^+$ at *m/z* 224, consistent to literatures.[46]

When the aldicarb concentration was at 0.02 mM (Figure 5(b)), the characteristic peak of aldicarb totally disappeared in the solutions treated with AQC functionalized membranes after 3 hours of UVA irradiation, and the peak intensity of aldicarb sulfoxide was visibly enlarged, indicating the pesticide was successfully oxidized and detoxified. While no significant changes were observed in the solution

of pure aldicarb and the one treated with pristine membranes. These results demonstrated the powerful oxidative functions of AQC functionalized PVA-*co*-PE nanofibrous membranes under UVA irradiation.

Conclusions

In this study, photo-induced self-decontaminating nanofibrous membranes were successfully prepared. Three PVA-*co*-PE polymers containing various ethylene content were fabricated into nanofibrous membranes, which were subsequently surface functionalized with a photo-active compound, anthraquinone-2-carboxylic acid. The morphologies of uniform nanofibers and open porous structures of prepared membranes were unchanged after the chemical reactions, and the immobilization of photo-active agents was confirmed by ATR-FTIR analysis and quantitatively evaluated. PVA-*co*-PE44-AQC membrane with a highly rough surface offered a higher hydroxyl group density and more immobilized AQC on membrane surfaces. PVA-*co*-PE27-AQC membrane with the lowest ethylene content provided more hydrogen donors of C-H bonds from secondary alcohol units to facilitate hydrogen peroxide generation. These AQC functionalized PVA-*co*-PE nanofibrous membranes exhibited excellent photo-induced antibacterial activities and efficient pesticide decontamination function against aldicarb, which demonstrated their great potential to serve as self-decontaminating materials.

Acknowledgements

This research was financially supported by National Textile Center (S06-CD01) and Defense Threat Reduction Agency (HDTRA1-08-1-0005). The author is grateful to Jastro-Shields Graduate

Student Research Fellowship Award at the University of California, Davis.

Reference

1. S. K. Obendorf, *AATCC Rev.,* 2010, **10**, 44-50.

2. H. L. Schreuder-Gibson, Q. Truong, J. E. Walker, J. R. Owens, J. D. Wander and W. E. Jones, *MRS Bulletin,* 2003, **28**, 574-578.

3. O. B. Koper, I. Lagadic, A. Volodin and K. J. Klabunde, *Chem. Mater.,* 1997, **9**, 2468-2480.

4. G. W. Wagner, O. B. Koper, E. Lucas, S. Decker and K. J. Klabunde, *J. Phys. Chem. B,* 2000, **104**, 5118-5123.

5. A. F. Bedilo, M. J. Sigel, O. B. Koper, M. S. Melgunova and K. J. Klabunde, *J. Mater. Chem.,* 2002, **12**, 3599-3604.

6. S. Rajagopalan, O. Koper, S. Decker, and K. J. Klabunde, *Chem. Eur. J.,* 2002, **8**, 2602-2607.

7. S. Sundarrajan, A. R. Chandrasekaran, and S. Ramakrishna, *J. Am. Ceram. Soc.,* 2010, **93**, 3955-3975.

8. P. W. Gibson, H. L. Schreuder-Gibson, and D. Rivin, *Colloids Surf. A,* 2011, **187-188**, 469-481.

9. P. W. Gibson, H. L. Schreuder-Gibson, and D. Rivin, *AIChE Journal,* 1999, **45**, 190-195.

10. H. L. Schreuder-Gibson, P. W. Gibson, K. Senecal, M. Sennett, J. Walker, W. Yeomans, D. Ziegler and P. P. Tsai, *J. Adv. Mat.,* 2002, **34**, 44-55.

11. S. S. Lee and K. S. Obendorf, *Fibers and polymers*, 2007, **8**, 501-506.

12. S. S. Lee and K. S. Obendorf, *J. Appl. Polym. Sci.,* 2006, **102**, 3430-3437.

13. S. S. Lee and K. S. Obendorf, *Text. Res. J.,* 2007, **77**, 696-702.

14. S. Sundarrajan, A. Venkatesan, and S. Ramakrishna, *Macromol. Rapid Commun.,* 2009, **30**,

1769-1774.

15. I. P. Parkin and R. G. Palgrave, *J. Mater. Chem.,* 2005, **15**, 1689-1695.

16. K. Tan and S. K. Obendorf, *J. Membr. Sci.,* 2007, **305**, 287-298.

17. K. Tan and S. K. Obendorf, *J. Membr. Sci.,* 2007, **289**, 199-209.

18. L. Chen, L. Bromberg, A. Hatton and G. Rutledge, *Polymer*, 2007, **48**, 4675-4682.

19. L. Chen, L. Bromberg, A. Hatton and G. Rutledge, *Polymer,* 2008, **49**, 1266-1275.

20. L. Chen, L. Bromberg, H.L. Schreuder-Gibson, J. Walker, A. Hatton and G. Rutledge, *J. Mater. Chem.,* 2009, **19**, 2432-2438.

21. L. Chen, L. Bromberg, J. A. Lee, H. Zhang, H. Schreuder-Gibson, P. Gibson, J. Walker, P. Hammond, A. Hatton, and G. Rutledge, *Chem. Mater.,* 2010, **22**, 1429-1436.

22. J. Zhu, Q. Bahramian, P. Gibson, H. Schreuder-Gibson and G. Sun, *J. Mater. Chem.,* 2012, **22**, 8532-8540.

23. M. R. Hoffmann, S. T. Martin, W. Y. Choi and D. W. Bahnemann, *Chem. Rev.,* 1995, **95**, 69-96.

24. E. Santala, M. Kemell, M. Leskel and M. Ritala, *Nanotechnology,* 2009, **20**, 035602.

25. J. A. Lee, K. C. Krogman, M. L. Ma, R. M. Hill, P. T. Hammond and G.C. Rutledge, *Adv. Mater.,* 2009, **21**, 1252-1256.

26. H. Q. Liu, J. X. Yang, J. H. Liang, Y. X. Huang and C. Y. Tang, *J. Am. Ceram. Soc.,* 2008, **91**, 1287-1291.

27. S. Sundarrajan and S. Ramakrishna, *J. Mater. Sci.,* 2007, **24**, 8400-8407.

28. N. L. Lala, R. Ramaseshan, B. J. Li, S. Sundarrajan, R. S. Barhate, Y. J. Liu and S. Ramakrishna, *Biotechnol. Bioeng.,* 2007, **42**, 8400-8407.

29. J. Zhu and G. Sun, *J. Mater. Chem.,*2012, **22**, 10581-10588.

30. N. Liu and G. Sun, *Ind. Eng. Chem. Res.,* 2011, **50**, 5326-5333.

31. N. Liu and G. Sun, *Dyes Pigm.,* 2011, **91**, 215-224.

32. N. Liu and G. Sun, *ACS Appl. Mater. Interfaces,* 2011, **3**, 1221-1227.

33. J. Y. Zhuo and G. Sun, *ACS Appl. Mater. Interfaces,* 2013, **5**, 10830–10835.

34. D. Wang, G. Sun, and B. S. Chiou, *Macromol. Mater. Eng.,* 2007, **292**, 407-414.

35. J. Luo, C. Pardin, W. D. Lubell and X. X. Zhu, *Chem. Commun.,* 2007, **21**, 2136-2138.

36. N. Liu, G. Sun and J. Zhu, *J. Mater. Chem.,* 2011, **21**, 15383-15390.

37. D. Wang, W. L. Xu, G. Sun and B. S. Chiou, *ACS Appl. Mater. Interfaces,* 2011, **3**, 2838-2844.

38. M. E. Avramescu, W. F. C. Sager, M. H. V. Mulder and M. Wessling, *J. Membr. Sci.,* 2002, **210**, 155-173.

39. J. Zhu, J. Yang and G. Sun, *J. Membr. Sci.,* 2011, **385-386**, 269-27619.

40. J. Zhu and G. Sun, *React. Funct. Polym.*, 2012, **72**, 839-845.

41. J. Zhu and G. Sun, *ACS Appl. Mater. Interfaces,* 2014, **6**, 925-932.

42. L. A. Gribov, O. B. Zubkova and A. A. Sigarev, *J. Struct. Chem.,* 1993, **34**, 147-154.

43. I. N. Juchnovski and T. M. Kolev, *Spectrosc. Lett.,* 1986, **19**, 1183-1193.

44. J. Zhu and G. Sun, *AATCC Rev.,* 2011, **11**, 59-64.

45 X. Fei, P. F. Gao, T. Shibamoto and G. Sun, *Arch. Environ. Contam. Toxicol.,* 2006, **51**, 509-514.

46. V. Dixit, J. C. Tewari and S. K. Obendorf, *J. Chromatogr. A,* 2009, **1216**, 6394-6399.

List of legends

Scheme 1. AQC immobilization onto PVA-*co*-PE nanofibrous membranes (Step1: AQC activation by CDI; Step2: esterification between activated AQC and PVA-*co*-PE nanofibrous membranes).

Scheme 2. The mechanism of photo-induced reactions of immobilized AQC on PVA-*co*-PE nanofibrous membranes.

Figure 1. SEM images of pristine PVA-*co*-PE nanofibrous membranes with (a) 27 mol%, (b) 32 mol%, (c) 44 mol% ethylene unit, and AQC functionalized PVA-*co*-PE nanofibrous membranes with (d) 27 mol%, (e) 32 mol%, (f) 44 mol% ethylene units (scale bar = 5um).

Figure 2. ATR-FTIR spectra of AQC compound, pristine PVA-*co*-PE nanofibrous mat with 27 mol% ethylene unit and (c) AQC functionalized PVA-*co*-PE nanofibrous membranes with 27 mol% ethylene unit (PVA-*co*-PE27-AQC).

Figure 3. The amount of immobilized AQC compound and measured (formed) H_2O_2 on PVA-*co*-PE nanofibrous membranes.

Figure 4. Figure 5. Antibacterial test results of *E. coli* (top) and *S. aureus* (bottom) treated with pristine PVA-*co*-PE nanofibrous membranes (left) and PVA-*co*-PE27-AQC (right) after 60min contact time.

Figure 5. HPLC results of pure aldicarb, aldicarb solutions treated with pristine and AQC functionalized PVA-*co*-PE nanofibrous membranes with (a) aldicarb concentration at 0.2 mM (b) aldicarb concentration at 0.02 mM.

Figure 6. Mass spectra results of (a) aldicarb at RT 13.14 min; (b) aldicarb sulfoxide at RT 5.41 min

Table 1. Table 1. Bacterial Reduction (%) caused by AQC functionalized nanofibrous membranes under different UVA exposure time.

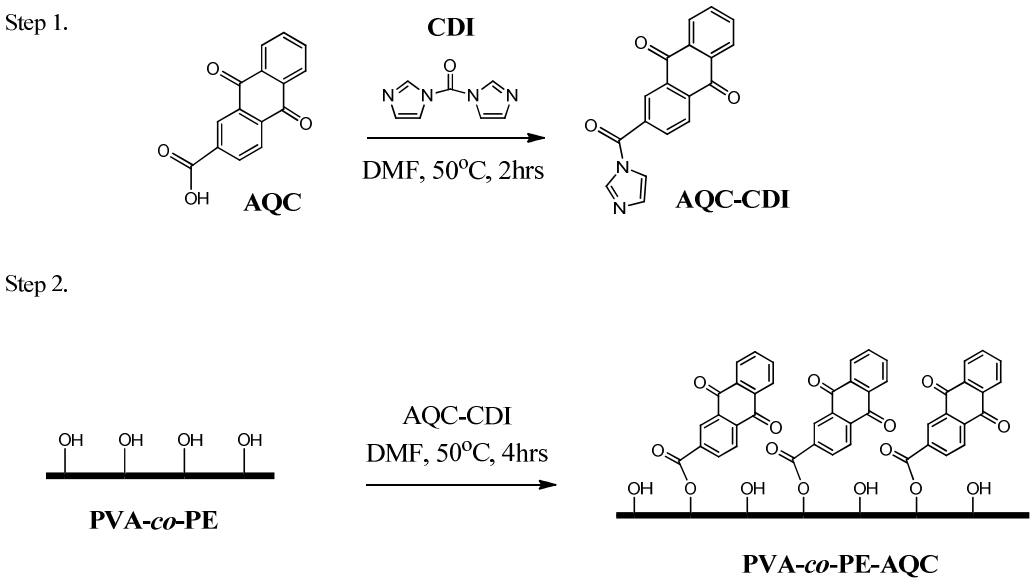

Scheme 1. AQC immobilization onto PVA-*co*-PE nanofibrous membranes (Step1: AQC activation by CDI; Step2: esterification between activated AQC and PVA-*co*-PE nanofibrous membranes).

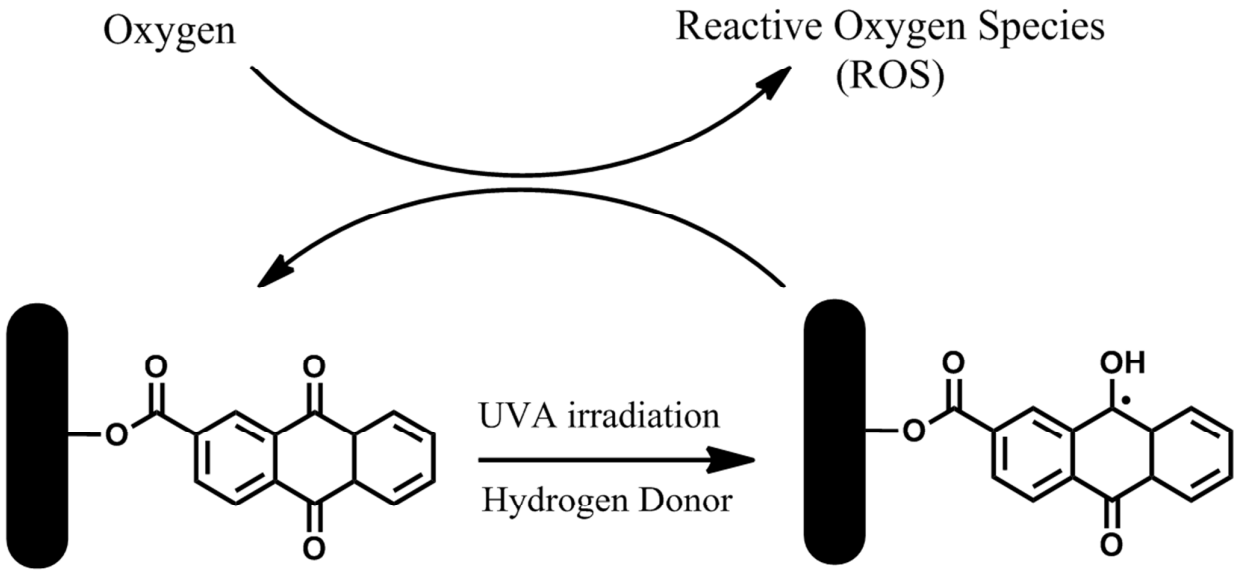

Scheme 2. The mechanism of photo-induced reactions of immobilized AQC on PVA-*co*-PE nanofibrous membranes.

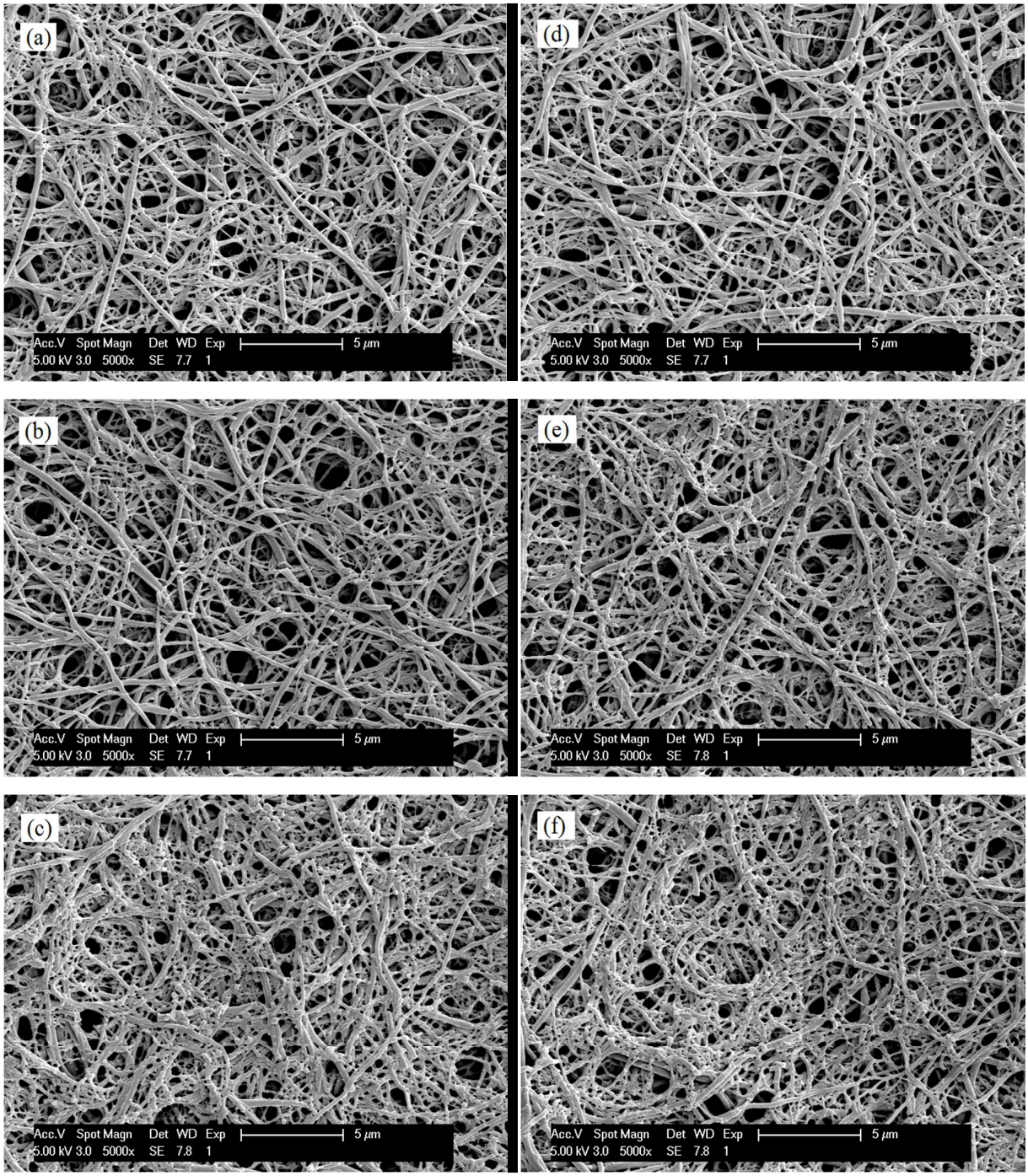

Figure 1. SEM images of pristine PVA-*co*-PE nanofibrous membranes with (a) 27 mol%, (b) 32 mol%, (c) 44 mol% ethylene unit, and AQC functionalized PVA-*co*-PE nanofibrous membranes with (d) 27 mol%, (e) 32 mol%, (f) 44 mol% ethylene units (scale bar = 5um).

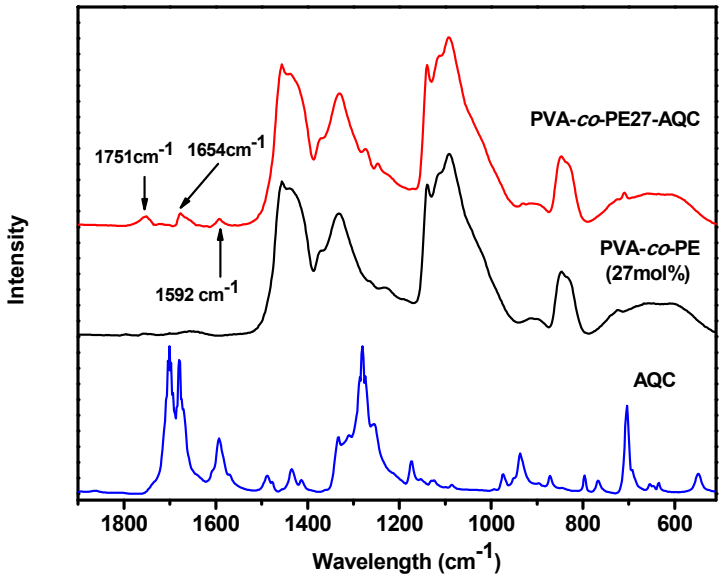

Figure 2. ATR-FTIR spectra of AQC compound, pristine PVA-*co*-PE nanofibrous membranes with 27 mol% ethylene unit and (c) AQC functionalized PVA-*co*-PE nanofibrous membranes with 27 mol% ethylene unit (PVA-*co*-PE27-AQC).

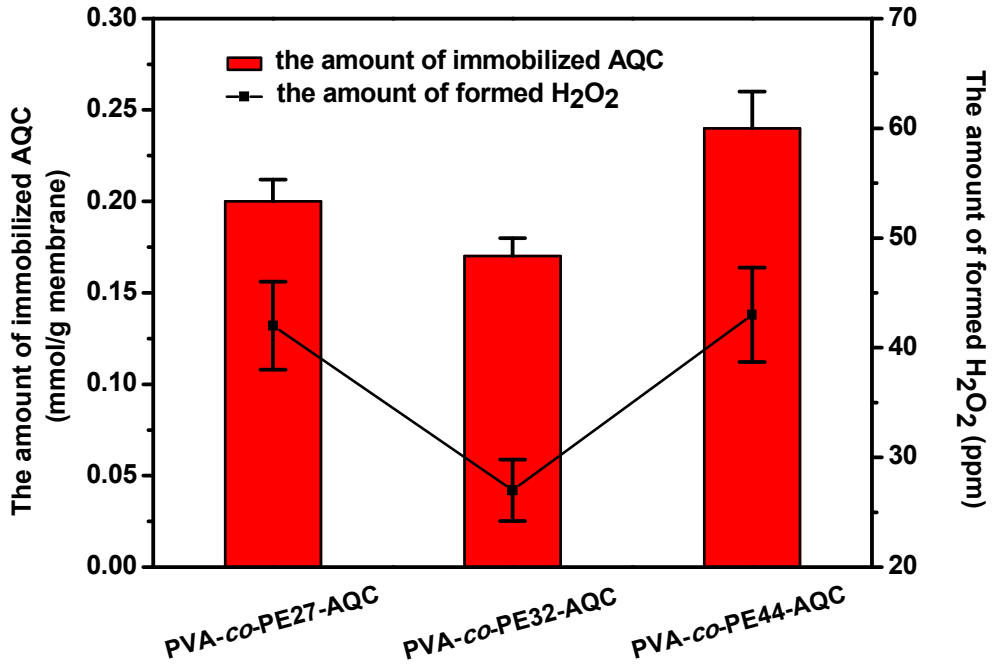

Figure 3. The amount of immobilized AQC compound and measured (formed) H_2O_2 on PVA-*co*-PE nanofibrous membranes.

Table 1. Bacterial Reduction (%) caused by AQC functionalized nanofibrous membranes under different UVA exposure time.

Bacterium	*S. aureus*		*E. coli*	
Exposure time	30 min	60 min	30 min	60 min
PVA-*co*-PE27-AQC	87.623	>99.999	80.443	>99.999
PVA-*co*-PE32-AQC	86.893	>99.999	78.012	>99.999
PVA-*co*-PE44-AQC	87.920	>99.999	82.375	>99.999

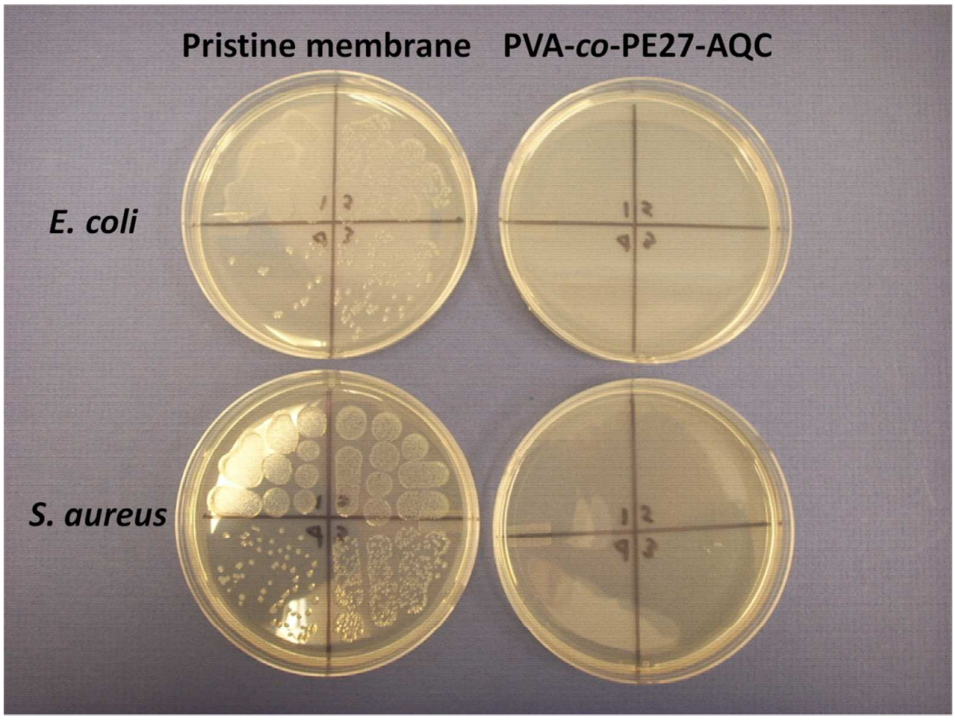

Figure 4. Antibacterial test results of *E. coli* (top) and *S. aureus* (bottom) treated with pristine PVA-*co*-PE nanofibrous membranes (left) and PVA-*co*-PE27-AQC (right) after 60min contact time.

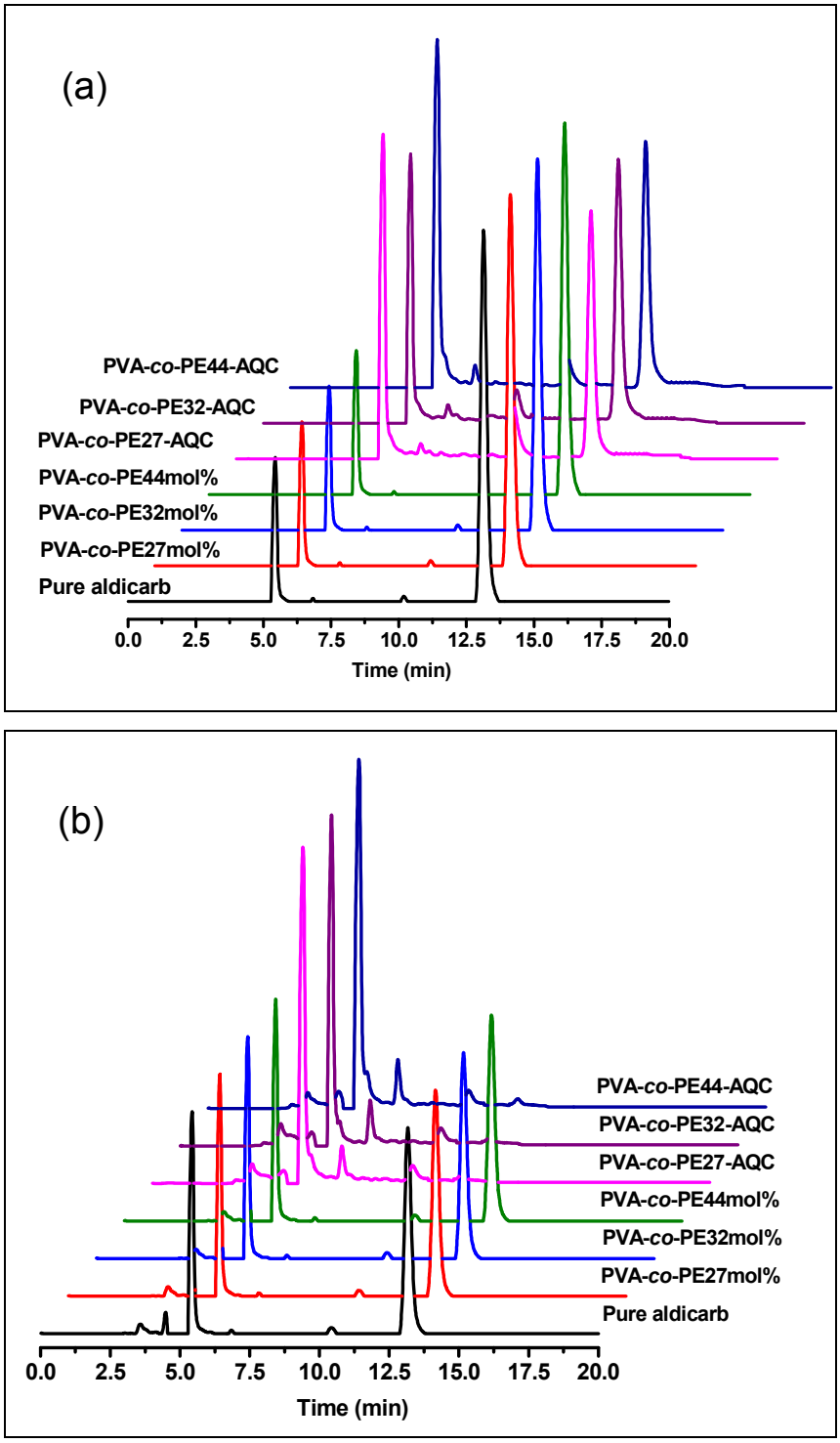

Figure 5. HPLC results of pure aldicarb, aldicarb solutions treated with pristine and AQC functionalized PVA-*co*-PE nanofibrous membranes with (a) aldicarb concentration at 0.2 mM (b) aldicarb concentration at 0.02 mM.

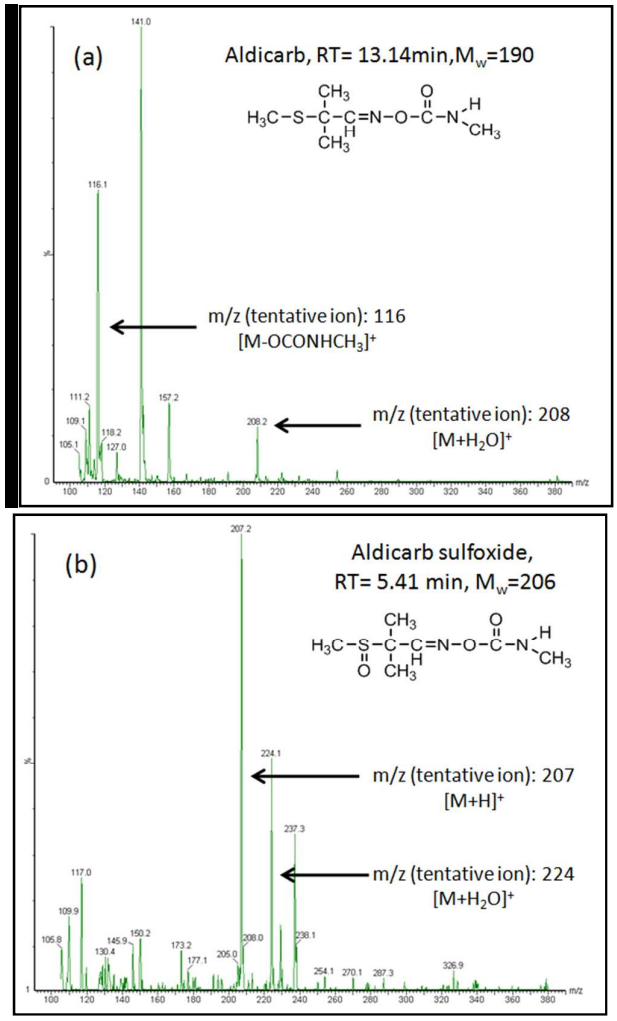

Figure 6. Mass spectra results of (a) aldicarb at RT 13.14 min; (b) aldicarb sulfoxide at RT 5.41 min.

Graphic Abstract

In this paper, hydrophilic nanofibrous membranes with photo-induced self-cleaning functionals were successfully prepared by covalently incorporating a organic photo-active compound, anthraquinone-2-carboxylic acid (AQC) onto poly(vinyl alcohol-*co*-ethylene) (PVA-*co*-PE) nanofibrous membranes. Under UVA irradiation, these AQC modified nanofibrous membranes are capable to generate reactive oxygen species (ROS), which attributes to the observed photo-induced chemical and biological decontamination functions..